

## Article

# Investigation on the Performance of Fire and Smoke Suppressing Asphalt Materials for Tunnels

Jiaquan Li <sup>1</sup>, Fei Liu <sup>1</sup>, Mingjun Hu <sup>1,\*</sup>, Changjun Zhou <sup>1</sup>, Liujiyuan Su <sup>1</sup> and Peng Cao <sup>2</sup>

<sup>1</sup> School of Transportation & Logistics, Dalian University of Technology, No. 2 Linggong Street, Dalian 116023, China; jiaquan123123@163.com (J.L.)

<sup>2</sup> College of Architecture, Civil and Transportation Engineering, Beijing University of Technology, Beijing 100124, China

\* Correspondence: humj@dlut.edu.cn

**Abstract:** The volatilization of asphalt fumes not only affects the health of construction workers, but also damages the environment. It even affects the construction quality of asphalt pavement in tunnels. This article focuses on solving the emission of asphalt fumes to better protect human health and the environment, while satisfying the use of asphalt pavement. A flame retardant and smoke suppressant (compound) with Mg(OH)<sub>2</sub> as the main component was developed, and flame retardant asphalt mixture and asphalt mastics were prepared to evaluate the flame retardant and smoke suppressant properties and performance effects. Firstly, its low- and high-temperature performances were investigated with BBR and DSR, respectively. Then, the indoor combustion test and the cone calorimeter test were used to evaluate the fire retardant smoke suppression effect of the asphalt mastic. Thirdly, the flame retardant effect of asphalt mastic mixed with the compound was further analyzed by the TG test and SEM. The pyrolysis temperature, mass loss, and microscopic state of the asphalt surface were used to verify and explain the flame retardant reaction effect and process of the compound. Finally, the asphalt mixture performance was evaluated, as well as the flame retardant smoke suppression effect by asphalt mixture combustion tests. The results showed that the flame retardant smoke suppression time of the flame retardant asphalt mixture was reduced by 66%, and the smoke emission area was reduced by 20%. The flame retardant smoke suppression effect of the asphalt mixture was improved by 44%. It is proven that this kind of fire retardant and smoke suppressing asphalt mastic and mixture met performance needs in use, and the fire retardant and smoke suppressing effect was obvious. This solution addresses the issue of asphalt smoke generated during the construction of asphalt pavement, providing better support for the construction of asphalt pavement in tunnels.

**Keywords:** asphalt mastic; asphalt mixture; flame retardant; smoke suppressant; performance



**Citation:** Li, J.; Liu, F.; Hu, M.; Zhou, C.; Su, L.; Cao, P. Investigation on the Performance of Fire and Smoke Suppressing Asphalt Materials for Tunnels. *Processes* **2023**, *11*, 3038. <https://doi.org/10.3390/pr11103038>

Academic Editor: Carlos Sierra Fernández

Received: 27 September 2023

Revised: 16 October 2023

Accepted: 20 October 2023

Published: 23 October 2023



**Copyright:** © 2023 by the authors. Licensee MDPI, Basel, Switzerland. This article is an open access article distributed under the terms and conditions of the Creative Commons Attribution (CC BY) license (<https://creativecommons.org/licenses/by/4.0/>).

## 1. Introduction

Aiming at the practical needs of engineering and environmental protection, there is an urgent need to develop a simple and effective fire retardant asphalt mixture to be applied to asphalt pavements. The roles of flame retardant and smoke suppression serve a dual purpose: on the one hand, to ensure the health of construction workers; on the other hand, to protect the environment. Simultaneously, it aims to achieve the pavement use requirements.

With the rapid development of tunnel construction, tunnel safety has attracted the attention of pavement researchers all over the world [1]. Tunnels are characterized by poor lighting, large longitudinal slopes, poor ventilation, and limited space for activities, so the toxic fumes generated by the asphalt mixture in paving will gather in large quantities, which seriously affects the health of construction workers and the quality of asphalt pavement paving [2]. Asphalt fumes mainly contain polycyclic aromatic hydrocarbons and a small

amount of oxygen, nitrogen, and sulfur heterocyclic compounds, as well as more than 100 kinds of organic substances such as naphthalene, phenanthrene, phenol, carbazole, pyridine, pyrrole, indole, and indene. Benzo(a)pyrene and other compounds are not only strong carcinogens, but also cause different degrees of pollution and damage to the natural environment, such as surface water, groundwater, atmosphere, and soil [3]. Asphalt pavement ignited by traffic accidents in tunnels is not only fiery, but also produces a large amount of asphalt smoke. In fires caused by asphalt combustion, 85% of the casualties die from asphyxiation due to inhalation of noxious gases rather than being burned to death [4,5].

Liu et al. [6] found that flame retardants reduced combustion and smoke, and the structural integrity of flame retarded asphalt mixtures after combustion was superior to that of virgin asphalt mixtures [7]. Liu et al. [8] prepared a flame retardant modified SBS asphalt, and the results showed that the peak exothermic rate was reduced by 4.02 kw/m<sup>2</sup> with the addition of 12% of the flame retardant compared to that without the flame retardant. Qiu et al. [9] found that the asphalt pavement temperatures above 330 °C promote the development of combustion. The experimental results of Yuan et al. [10] showed that the burning degree of fire retardant asphalt mixtures was lower than that of virgin asphalt mixtures. Li et al. [11] demonstrated that the fire retardant effectively shortened the combustion time of the asphalt mixtures, and the surface temperatures and stability of the residue after combustion were also reduced. Qin et al. [12] found that the split strength ratios were the same before and after combustion, while the freeze–thaw split strength ratios were reduced after combustion, which verified the fire retardant properties of fire retardant asphalt mixtures.

Inorganic phosphorus-based flame retardants are efficient and nontoxic, but are not compatible with water molecules and are prone to spontaneous combustion [13]. Organic halogen-based flame retardants emit toxic and corrosive gases during the flame retardant process, and were proved to be not environmentally friendly, while nitrogen-based flame retardants have poor flame retardant effects [14]. The organosilicon and organophosphorus systems mostly perform as modifiers and plasticizers, but are not used widely as flame retardant components in asphalt mixtures [15]. Magnesium hydroxide has become one of the most popular halogenated flame retardant alternatives due to its good stability, nontoxicity, and smoke inhibition properties. There is a trend to develop low-dose flame retardants to balance the flame retardant properties with the pavement performance of asphalt mixtures [11]. Hu et al. [16] found that the alkaline mixture has good smoke suppression effects, does not affect the performance and construction process of asphalt pavement, and is suitable for pavement materials. Qin et al. [17] and Li et al. [18] found that the incorporation of magnesium hydroxide flame retardant can improve high-temperature performance and reduce low-temperature performance of asphalt mixtures by conventional performance and rheological tests, but has little effect on water stability. Thus, they demonstrated that the use of flame retardant in asphalt mixtures is feasible. Cong et al. [19] studied the effect of adding of flame retardants on the physicochemical properties of asphalt, and found that the addition of 6% flame retardants could reduce the heat released from asphalt in the temperature range of 195 °C to 600 °C. Tan et al. [20] used 1% kaolin and 8% traditional flame retardants to enhance flame retardant efficiency of traditional flame retardants, while weakening low-temperature performance asphalt mixtures. Zhou et al. [21] investigated the influence of different types and dosages of flame retardants on the performance of flame retardant asphalt. The results revealed that the flame retardants enhanced the intermolecular forces of the flame retardant asphalt, thereby improving its performance. However, increasing the dosage of the flame retardants did not enhance the thermal stability of the flame retardant asphalt. Yu et al. [22] analyzed the effect of flame retardants on the high- and low-temperature properties of asphalt. The results showed that the rutting factor of asphalt increased, and the high-temperature performance of asphalt was improved with the increase of flame retardant dosage. However, it has a negative effect on the low-temperature performance, and it is suggested that the reasonable

dosage is 8%. Yu et al. [23] evaluated the stability, indirect tensile strength, and rutting resistance, and concluded that a certain hydroxide content had the most significant effect on improving the flame retardancy of asphalt. Bonati et al. [24] found that the use of magnesium hydroxide flame retardant filler instead of conventional mineral powders had a significant flame retardant effect on the heat-absorption decomposition and cooling of asphalt substrate at 200 °C and 300 °C. Zhu et al. [25] found that low doses of layered hydroxide can be well dispersed in asphalt, improving the resistance to thermal oxidation and densification of the coke layer, and reducing the burning rate of asphalt. Sheng et al. [26] studied composite halogen-free flame retardant asphalt mixtures with magnesium hydroxide, and found that the flame retardant not only reduced the amount of heat and carbon monoxide released during burning, but also validated the application of such materials in tunnels. From the asphalt mixture performance, Xu et al. [27] found that using magnesium hydroxide flame retardant to replace part of the mineral powder improved the thermal stability of asphalt and reduced the burning level of asphalt from FH-3 to FH-1 (burning difficulty level), without significantly reducing the original road performance of the asphalt mixture. Xia et al. [28] found that the molecular weight of the characteristic substances of soot and residue of asphalt mixtures after combustion was smaller after doping with fire retardant, and the effect of fire retardant was significant. Jiang et al. [29] investigated the performance of fire retardant asphalt under different aging conditions. In terms of fire retardant properties, SPR increased in the early stages of combustion, but decreased in the later stages of combustion. Xia et al. [30] explored the feasibility of fire retardant asphalt pavement in tunnels, and verified the fire retardant and smoke suppressive properties. It was shown that the flame retardant had good flame retardant properties at 6%. Lu et al. [31] found that 8% hydroxide flame retardant had better flame retardant effects. At the same time, the adhesive effect of the flame retardant means the oxidized flame retardant layer is more dense.

In this article, the cone calorimeter test and TG analysis were used to analyze the flame retardant properties of flame retardant asphalt mastics. At the same time, SEM was applied to observe the surface of the fire retardant asphalt mastic after high-temperature exposure to verify the fire retardant and smoke suppressing effect of the fire retardant asphalt mastic from a microscopic point of view. Additionally, DSR and BBR tests were also applied to investigate the rheological properties of fire retardant asphalt mastics. Finally, flammability tests were conducted on fire retardant asphalt mixtures to visually verify the effect of fire retardant smoke suppression, as well as to fully verify the water stability, high-temperature stability, and low-temperature performance of fire retardant asphalt mixtures.

This article highlights two perspectives on fire retardant and smoke suppression properties: fire retardant asphalt mastic, and fire retardant asphalt mixtures. A variety of test methods were applied to conduct the study. The study of fire retardant asphalt mastic and fire retardant asphalt mixtures, as a whole, is more convincing for the performance of the materials. It is fully demonstrated that fire retardant smoke suppression asphalt not only reduces the emission of asphalt smoke, but also that fire retardant asphalt mixtures meet the requirements for pavement use.

## 2. Raw Materials and Mix Design

Before conducting experimental studies, it was necessary to test the indicators of raw materials. The following tests were set up to better understand the properties of the raw materials in the test:

### 2.1. Asphalt

Panjin #90 virgin asphalt binder was used. The asphalt penetration test, ductility test, and softening point test were carried out with reference to “Standard Test Methods for Asphalt and Double-layer Asphalt Mixture in Highway Engineering JTG E20-2011”. The test methods referred to T0604-2011, T0605-2011, and T0606-2011, respectively, and the test

methods in this section refer to Section 3.1.1 of this document. The technical indicators are shown in Table 1.

**Table 1.** Technical specifications of virgin asphalt.

Testing Items	Specification Requirements	Test Results
Penetration (25 °C, 100 g, 5 s)/0.1 mm	80–100	89
Ductility (15 °C, 5 cm/min)/cm	≥100	≥150
Softening point/°C	≥44	45

### 2.2. Flame Retardant and Smoke Suppressant

The flame retardant and smoke suppressant was obtained from the Road Engineering Laboratory of Dalian University of Technology. XRD and XRF results of the specimens are shown in Figure 1 and Table 2. XRD and XRF were tested by the Analytical Testing Center of Dalian University of Technology. XRD was tested under wide-angle physical phase (5°~130°) conditions, and XRF was tested by compression flake method (5 g, particle size < 200 mesh, moisture content < 1%). XRD found that there is a peak at 10°~70°, so this section was selected as the analyzed data.

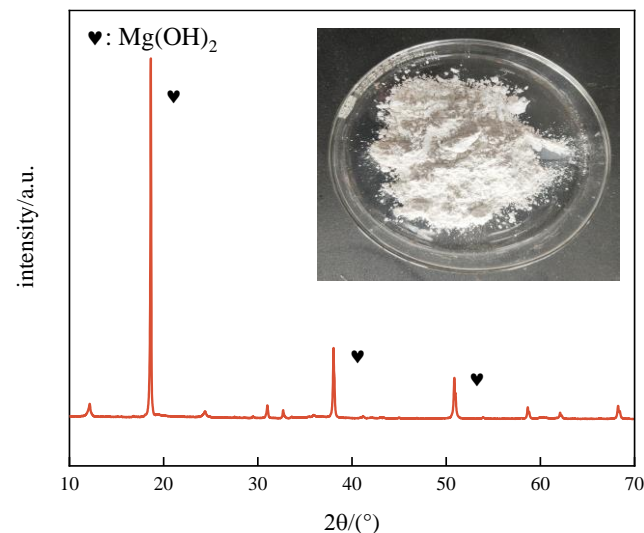


**Figure 1.** XRD diffraction pattern of flame retardant and smoke suppressant.

**Table 2.** Quantitative and qualitative analysis by XRF.

Compositions	Percentage (%)
MgO	77.6
SiO <sub>2</sub>	14.8
CaO	4
Other	3.6

The specimen was dried and then sieved through an 80-micron square hole sieve, and 5 g of powder was taken. For different crystals, the XRD spectra have diffraction peaks of different intensities at different angles  $\theta$  or energies  $E$ . Moreover, the number, position, intensity, and profile of the main diffraction peaks are the main information extracted and referenced when analyzing and comparing XRD spectra [32], and the three intensity peaks of this XRD diffraction pattern are all from Mg(OH)<sub>2</sub> crystals. XRF quantitative analysis shows that more than 77% of the component is Mg.

### 2.3. Mineral Powder

In this study, three types of mineral powders were selected. A is clayey mineral powder, B is limestone mineral powder, and C is granite mineral powder. Limestone is a

carbonate rock with calcite as the main component and is not very stiff. Kaolinite is mainly a product of natural alteration of feldspar and other silicate minerals. The main minerals in granite are quartz, potassium feldspar, and acidic plagioclase. The samples after sieving are shown in Figure 2.



**Figure 2.** Three types of mineral powder samples.

#### 2.4. Aggregate Gradation

In this study, three types of mineral powder (A, B, and C) and three grades of coarse basalt aggregates (0–5 mm, 5–10 mm, and 10–20 mm) were used to prepare the AC-16 asphalt mixture with 4.93% asphalt content. The proportions of aggregates were determined using synthetic grading, and the respective percentages are adjusted to ensure that the synthetic grading curves were in the middle of the upper and lower limits. The percentage of aggregates is shown in Table 3, and the synthetic grading curves are shown in Figure 3.

**Table 3.** AC-16 asphalt mixture ratio of each material grade.

Material Grade (mm)	Percentage (%)
10–20	22.6
5–10	10
0–5	62
Mineral powder	5.4

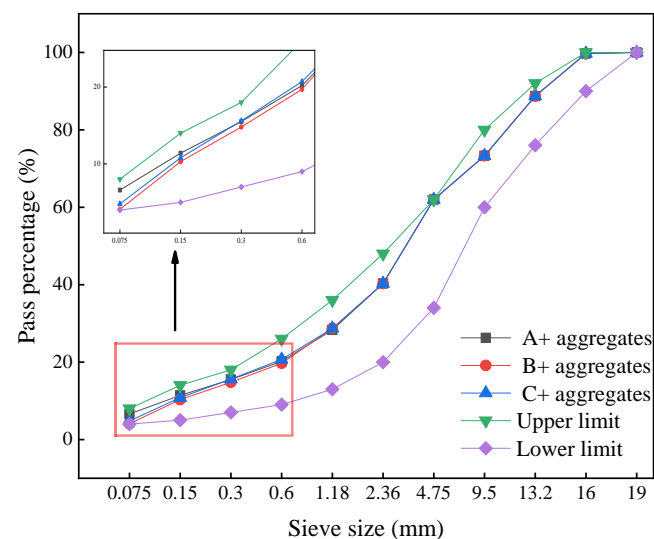


**Figure 3.** Aggregate gradation curves of AC-16 asphalt mixture.

### 3. Experimental Methods

Focusing on solving the problem of flame retardant and smoke suppression in asphalt mixtures, this study investigated flame retardant asphalt materials at multiple scales. The

following research experiments were carried out to study the flame retardant properties and pavement performance of asphalt mastic and asphalt mixtures.

### 3.1. Asphalt Mastics

The filler was sieved to less than 0.075 mm, and then mixed with asphalt to obtain asphalt mastic. Two filler/asphalt ratios of 1.0 and 1.1 [33], and five flame retardant contents of 6%, 7%, 8%, 10%, and 15% (the proportion of replacement mineral powder) were selected. Specimens were prepared, and experiments were performed following studies in accordance with the “Test Procedure for Asphalt and Asphalt Mixture for Highway Engineering JTG E20-2011”.

The method was referred to by Huang et al. [34] and Hu et al. [35] in the preparation of hydroxide flame retardant asphalt mastic. It was combined with the actual preparation method in this study, as follows:

① The flame retardant and mineral powder were dried in an oven at  $105 \pm 5 \text{ }^\circ\text{C}$  for about 1 h each. After weighing the test dosage, the rest was kept sealed. The virgin asphalt [36] was dehydrated in an oven at  $150 \pm 5 \text{ }^\circ\text{C}$  for 1 h. ② Flame retardants were added to the mineral powders at dosages of 6%, 7%, 8%, 10%, and 15% by mass of the mineral powders. The dried flame retardant and mineral powder mixtures were mixed into virgin bitumen at  $160 \pm 5 \text{ }^\circ\text{C}$  with reference to filler/bitumen ratios of 1.0 and 1.1. A test group was formed. ③ Started the high speed shear machine at 500 r/min agitation. After mixing, continuous shearing was carried out at 3000 r/min for 1 h. Then, sheared at 500 r/min for 5 min to remove air bubbles, during which the asphalt temperature is controlled at  $160 \pm 5 \text{ }^\circ\text{C}$ . ④ During the cooling process, the prepared flame retardant asphalt mastic was stirred manually with a stirring rod to prevent segregation during the cooling process. Then, the molds were poured to test the three main indicators of asphalt mastic.

#### 3.1.1. Asphalt Mastic Performance Test Methods

##### (1) Conventional performance tests

The conventional performance test referred to “Standard Test Methods for Asphalt and Asphalt Mixture in Highway Engineering JTG E20-2011”. Test methods refer to T0604-2011, T0605-2011, and T0606-2011, respectively.

The test schematic is shown in Figure 4. The test results are shown in Figure 3. Specific test operations were as follows:

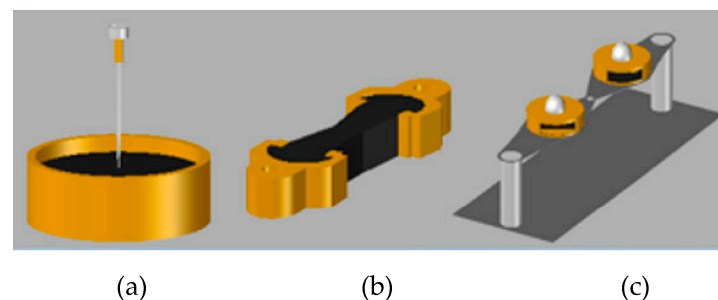


**Figure 4.** Conventional performance test schematic: (a) penetration test; (b) ductility test; (c) softening point.

##### a. Penetration test

The penetration test was used to evaluate the hardness and softness of fire retardant asphalt mastics. The mixed asphalt binder was poured into a small sample dish with an inner diameter of 55 mm and a depth of 35 mm. The sample dish containing the specimen was cooled at room temperature of  $15 \text{ }^\circ\text{C}$ ~ $30 \text{ }^\circ\text{C}$  for not less than 1.5 h, and then held in a constant temperature water bath at  $25 \text{ }^\circ\text{C} \pm 0.1 \text{ }^\circ\text{C}$  for not less than 1.5 h. The SYD-2801F

penetration degree tester and HWY-3 low-temperature constant temperature water bath tester were used.

b. Ductility test

Ductility mainly reflects the ductility and plasticity of the asphalt mastic. For each type of asphalt mastic, three specimens were prepared. Firstly, the mixed asphalt mastic was slowly injected into the standard test mold; the height of the specimen should be higher than test mold. The specimen was cooled at room temperature for at least 1.5 h, and then it was scraped flat. Then, put the test piece into the water tank at 25 °C for 1.5 h. The test piece was tested by the SYD-4508G-1 asphalt ductility tester. The distance of specimen stretching until breaking was defined as the ductility value.

c. Softening point test

The softening point mainly reflects the temperature sensitivity of the asphalt mastic. For each type of asphalt mastic, two specimens were prepared. The asphalt mastic was slowly injected into the standard mold, with the height of specimen higher than the mold. The specimen was cooled at room temperature for 30 min, and then scraped flat. The specimen was tested by the SYD-2806F instrument. The specimens gradually softened until they touched the bottom surface, and the average temperature (accurate to 0.5 °C) was regarded as the softening point indicator.

(2) Low-temperature rheological properties

The low-temperature rheological properties test referred to the “Standard Test Methods of Bitumen and Bituminous Mixtures for Highway Engineering JTG E20-2011” with T0627-2011. The low-temperature rheological properties responded to the flexural creep strength of asphalt mastic, which was a major influence on the low-temperature cracking of asphalt pavements.

The filler/asphalt ratio was determined to be 1.1 by the conventional tests described above. The amount of fire retardant and smoke inhibitor was determined by indoor combustion testing of fire retardant asphalt mastic. For each type of asphalt mastic, three specimens were prepared. The filler/asphalt ratio was 1.1. Two kinds of asphalt mastic were made with reference to the proportion of 0% and 7% fire retardant and smoke suppressant, and then mix asphalt mastic was slowly injected into the standard mold, with the height of the specimen higher than the mold. The size of the test piece was 6.35 mm × 12.7 mm × 127 mm, and the test temperature was −6 °C, −12 °C, and −18 °C. ① Specimens need to be kept at the test temperature for 60 ± 5 min. ② The contact load of the specimen was 35 ± 5 mN, load application time not more than 10 s. ③ Loading process: an initial load of 980 mN ± 50 mN was applied in 1 s. The load was reduced to 35 mN ± 10 mN and maintained for 20 s. ④ A load of 980 mN ± 50 mN was applied and maintained for 240 s. The load was removed and returned to a contact load of 35 mN ± 10 mN. The bending creep stiffness  $s$  and creep rate  $m$  of the asphalt mastic were tested using a BBR.

(3) High-temperature rheological properties

The high-temperature rheological properties test referred to the “Standard Test Methods of Bitumen and Bituminous Mixtures for Highway Engineering JTG E20-2011” with T0628-2011. High-temperature rheological properties responded to high-temperature rutting resistance of asphalt.

Both the temperature sweep test and the frequency sweep test were performed using a DSR. The filler/asphalt ratio was 1.1. Two types of asphalt mastics were prepared with 0% and 7% fire retardant and smoke suppressant ratios, respectively. The standard specimens of asphalt mastic were poured on silicone sheet molds with diameters of 25 mm and 8 mm, respectively.

The temperature sweep test was used to evaluate the high-temperature rheological properties of asphalt. The test was conducted over a temperature range of 46 °C to 82 °C,

at a frequency of 10 rad/s, in a strain-controlled loading mode with a strain level of 12% and a rotor diameter of 25 mm with a pitch of 1 mm. The frequency sweep test is used to characterize the rheological properties of asphalt materials. Test conditions: the test temperature range is 4~64 °C, with 12 °C as the interval, and the frequency range is 0.1~60 Hz. The loading mode was strain-controlled: at high temperatures (above and including 40 °C), using 25 mm rotors with a pitch of 1 mm, the strain level is 0.1%; at low temperatures (below 40 °C), using 8 mm rotors with a pitch of 2 mm, the strain level is 0.05%. The low-frequency (high-temperature) section was selected, and then the dynamic shear modulus was fitted with the 2S2P1D model. The 2S2P1D model contains two spring cells, two parabolic creep cells, and one viscous pot cell, and its expression contains seven parameters. The fitting results are shown in Figure 9. Expression for the complex shear modulus ( $G^*$ ) is given as follows in Equation (1):

$$G^* = G_e + \frac{G_g - G_e}{1 + \alpha(i\omega\tau_0)^{-k} + (i\omega\tau_0)^{-h} + (i\omega\beta\tau_0)^{-1}} \quad (1)$$

where

$G_e$  represents the equilibrium modulus,  $\omega$  converges to 0;

$G_g$  represents the glassy modulus,  $\omega$  converges to  $\infty$ ;

$\alpha$ ,  $k$ , and  $h$  are three constants,  $0 < k < h < 1$ ;

$\beta$  is a constant;

$\tau_0$  represents the characteristic time.

### 3.1.2. Evaluation of Flame Retardant and Smoke Suppressing Effect

#### (1) Indoor combustion test

In order to determine the dosage of flame retardant and smoke suppressant, an indoor combustion test was used. The fire retardant and smoke suppressing effects of virgin asphalt, virgin asphalt mastic, and fire retardant asphalt mastic with different dosages of fire retardant and smoke suppressing agents were investigated separately.

The mixed flame retardant asphalt mastic was poured into a small sample tray with an inner diameter of 55 mm and a depth of 35 mm at a height of 2/3. Flame retardant asphalt mastic samples were made at 6%, 7%, 8%, 10%, and 15% mineral powder replacement ratios at a filler/asphalt of 1.1.

Indoor combustion was ignited by a gas burner [37], the ignition time of each group of asphalt mastic was 10 s, the mass of asphalt mastic was 25 g, and the combustion exposure area was consistent. In image processing, set the time point 10 s after ignition to 0 time point. Set the time interval to 1 or 2 s until no more smoke is produced. The image processing software unified the image specification as  $3.49 \times 2.25$  pixels/inch, and set the grid division as  $10 \text{ mm} \times 10 \text{ mm}$ , so that the smoke area of a certain moment can be obtained through software processing. Through the imaging equipment, the whole burning process of flame retardant asphalt mastic was captured. The schematic is shown in Figure 5.

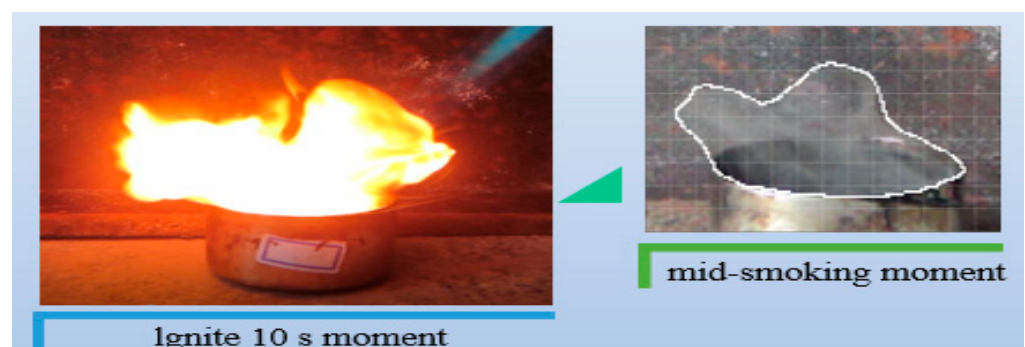


Figure 5. Indoor combustion test and image processing.

## (2) Cone calorimeter test

The smoke production rate of asphalt mastic containing 7% and 0% flame retardant and smoke suppressant was further tested by a cone calorimeter. Two separate asphalt mastic specimens were prepared according to the filler/asphalt ratio of 1.1. The size was 100 mm × 100 mm × 5 mm, and the specimens were placed in the center of the conical calorimeter specimen table, and the conical heater was lowered onto the specimens. The most important parameter index was tested, namely, SPR. SPR more directly and accurately reflects the effect of flame retardant and smoke suppression. The test results are shown in Figure 12.

Test procedure: ① Mounted the conical calorimeter and probe on the base. Calibrated the length and sensitivity of the probe. ② Put the prepared asphalt sample into the conical calorimeter. ③ The heat flux parameter was set to 35 kW/m<sup>2</sup>, and the temperature was 300 °C. ④ Started the test, and collected SPR data.

## (3) Thermogravimetric analysis

TG tests were conducted for two doses of asphalt mastic with the determined amount of 7% flame retardant smoke suppressant and 0% flame retardant smoke suppressant. TG data can be analyzed for heat-absorption temperature characteristics of flame retardants in fire retardant asphalt mastics, residuals, and mass loss rates during the combustion phase.

Test operation steps: ① Placed the asphalt mastic specimen in the sample disk. ② Set parameters: flow rate of 210 mL/min. Test temperature was 30 °C–800 °C, and the heating rate was 10 °C/min. One g of each of the two doping asphalt mastics was taken as a specimen. ③ Closed the sample compartment door and started the instrument to begin thermogravimetric analysis. The instrument will automatically raise and lower the temperature and record mass changes according to the set parameters. The test results are shown in Figure 13.

## (4) Microscopic analysis of flame retardant asphalt mastic.

SEM was used to observe the asphalt mastic mixed with two fire retardant and smoke suppressant compounds from a microscopic point of view. Four samples were divided into two groups: one group of surfaces treated by flame (about 300 °C) combustion, and the other group of samples tested by TG (max. temperature 800 °C).

Test procedure: ① The surface of asphalt mastic must be uniformly sprayed with alloy film to enhance electrical conductivity. ② Placed the treated asphalt sample on the sample stage and fixed it with conductive adhesive to ensure that a clear image was obtained. ③ In this test, the adjustment voltage was 10 kV, the focal length and contrast, etc., were adjusted according to the specimen. ④ Acquired the scanned image for calibration.

At different temperatures, changes in the state of the flame retardant and smoke suppressant compound particles encapsulated on the surface of the asphalt mastic were observed, verifying the flame retardant and smoke suppressant effect of the flame retardant asphalt mastic. The images are shown in Figures 14 and 15.

### 3.2. Asphalt Mixture

The asphalt mixes in this study were prepared as follows: ① Placed the virgin asphalt into an electric oven and kept it at 140 ± 5 °C for 1.5 h. Mineral powder and flame retardant and smoke suppressant compound were kept dry at 105 °C. ② Used the ratio of aggregate, put the prepared aggregate into the asphalt aggregate mixer and mixed it well, maintained at 150 ± 5 °C for 1 h. ③ Asphalt content was 4.93%, took a certain amount of virgin asphalt, poured it into the mixer and mixed it fully for 90 s. ④ Then, the mineral powder and the corresponding proportion of the flame retardant and smoke suppressant compound were poured into the mixing pot and mixed thoroughly for 90 s. ⑤ Specimens were made under mixing temperature conditions.

### 3.2.1. Asphalt Mixture Performance Test

This section for flame retardant asphalt mixture molding, testing, and other requirements refers to the “Standard Test Methods of Bitumen and Bituminous Mixtures for Highway Engineering JTG E20-2011” regulations.

#### (1) Marshall stability and flow value

The flow value and stability responded primarily to the mix design of the asphalt mixture. The mixing temperature was  $150 \pm 5$  °C, asphalt content was 4.93%, filler/asphalt was 1.1, and the mineral powder and aggregate were mixed well. Each mineral powder was 1 group, each group was 4 specimens, and a total of three groups were prepared. The test referred to the “Standard Test Methods of Bitumen and Bituminous Mixtures for Highway Engineering JTG E20-2011” with T0709-2011. The data were analyzed in Figure 16.

#### (2) Water stability

The water stability test referred to the “Standard Test Methods of Bitumen and Bituminous Mixtures for Highway Engineering JTG E20-2011” with T0729-2000. Asphalt mixture freeze–thaw splitting test was used to evaluate the water stability of asphalt mixture. The flow value and stability respond primarily to the mix design of the asphalt mixture. The Marshall compaction method was used to form the 8 standard duplicated specimens: the number of compactions for each side of 50 times, asphalt content was 4.93%, filler/asphalt was 1.1, and flame retardant alternative mineral powder content was 7%. The specimens were randomly divided into a control group and a test group, and each group had 4 duplicated specimens.

① The test group was completely immersed in water, and filled with water under vacuum conditions. The vacuum was maintained at 97.3–98.7 kPa for 15 min, and the specimens were immersed in water for 0.5 h after pressure was restored. ② The specimens were tested in a plastic bag, about 10 mL of water was added, and the bag was tightened. ③ The packaged specimens were then placed in a refrigerator at a freezing temperature of  $-18 \pm 2$  °C for  $16 \pm 1$  h. ④ Then, specimens were placed in a thermostatic water bath at  $60 \pm 0.5$  °C for 24 h. The two groups of specimens were immersed in a constant temperature bath of  $25 \pm 0.5$  °C over 2 h. ⑤ The specimen was placed on the mold with a loading rate of 50 mm/min, and a load not exceeding 30 N, until the specimen was destroyed and the data recorded. The data were analyzed in Figure 17.

The splitting test was carried out by UTM-100. Water stability was calculated by the following Equation (2):

$$TSR = \frac{\bar{R}_{T2}}{\bar{R}_{T1}} \times 100 \quad (2)$$

where

$TSR$  represents the ratio of freeze–thaw splitting strength at T1 and T2 (%);

$\bar{R}_{T2}$  represents average value of splitting tensile strength (MPa) of the second group of valid specimens after freeze–thaw cycles;

$\bar{R}_{T1}$  represents average value of splitting tensile strength (MPa) of the first group of valid specimens without freeze–thaw cycles.

#### (3) High-temperature stability

High-temperature stability of this asphalt mixture was tested by the asphalt mixture rutting test. The method referred to the “Standard Test Methods of Bitumen and Bituminous Mixtures for Highway Engineering JTG E20-2011” with T0719-2011. The test was to determine the high-temperature rutting resistance of the flame retardant mix. The data were analyzed in Figure 17.

The protocol of asphalt mixture with the rutting test was used to evaluate the high-temperature stability of the asphalt mixture. In this study, the size of the rutted plate is 300 mm × 300 mm × 50 mm, and the compaction density of the mixture should meet the requirements of the Marshall standard specimen.

① Then, the specimens were placed in a constant temperature box at  $60 \pm 5^\circ\text{C}$  for 3 h. ② The contact pressure between the test wheel and the specimen was adjusted to  $0.7 \pm 0.05\text{ MPa}$ . ③ Started the automatic rutting tester. The rutting deformation  $d_1$  and  $d_2$  at 45 min ( $t_1$ ) and 60 min ( $t_2$ ) were measured after heat preservation, as required (accurate to 0.01 mm). Dynamic stability was calculated by the following Equation (3):

$$DS = \frac{(t_1 - t_2) \times N}{d_1 - d_2} \times C_1 \times C_2 \quad (3)$$

where

$DS$  represents dynamic stability (times/mm);

$d_1, d_2$  represent deformation (mm) corresponding to time  $t_1, t_2$ , respectively;

$C_1$  and  $C_2$  equal to 1.0;

$N$  is 42 (times/mm).

#### (4) Low-temperature stretchability

Low-temperature stability of this asphalt mixture was tested by the asphalt mixture bending test. The method referred to the "Standard Test Methods of Bitumen and Bituminous Mixtures for Highway Engineering JTG E20-2011" with T0715-2011. Asphalt mixture low-temperature bending beam test was used to evaluate the mechanical properties of hot mix asphalt mixture bending damage at the specified temperature and loading rate.

The experimental conditions were as follows: ① The test temperature was  $-10 \pm 0.5^\circ\text{C}$ , the loading speed was 50 mm/min, and the specimen dimensions were  $250 \pm 2.0\text{ mm}$  in length,  $30 \pm 2.0\text{ mm}$  in width, and  $35 \pm 2.0\text{ mm}$  in height. ② After the specimens were made, specimens were kept at a constant temperature of  $-10 \pm 0.5^\circ\text{C}$  for 45 min. ③ The specimen was immediately and symmetrically secured on the support with the force and displacement transducers set to zero, and loaded at a rate of 50 mm/min; number of specimens not less than 4. ④ After meeting the test conditions, the test was completed on the UTM-100 until the specimens were broken. The data were analyzed in Figure 17.

The modulus of bending strength was calculated by the following Equation (4):

$$S_B = \frac{R_B}{\varepsilon_B} \quad (4)$$

where

$S_B$  represents modulus of bending strength (MPa);

$R_B$  represents bending and tensile strength (MPa);

$\varepsilon_B$  represents maximum bending tensile strain ( $\mu\varepsilon$ ).

#### 3.2.2. Evaluation Tests for Flame Retardant and Smoke Suppressing Effect

Two Marshall specimens containing different amounts of flame retardant and smoke suppressant compounds (0%, 7%) were made separately for combustion tests.

① Placed the burning isolation plate on the electronic scale and set the scale to zero. ② Placed the test piece on the isolation plate and sprayed 30 g of gasoline evenly. ③ Ignite the gasoline. Mass loss was recorded at 30 s, 60 s, 90 s, 120 s, and 150 s until the end of combustion.

According to the mass loss at different moments, the change rule of the data analysis is shown in Figure 18. Evaluate the flame retardant and smoke suppression effect of flame retardant asphalt mixtures.

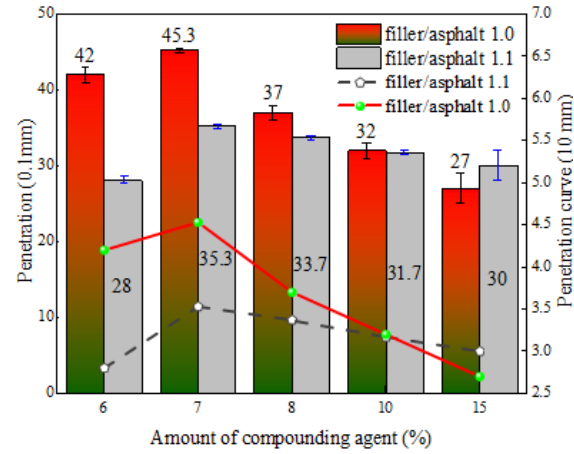
## 4. Results and Discussion

The test data, graphs, and charts obtained by the set test methods were developed in order to analyze the following.

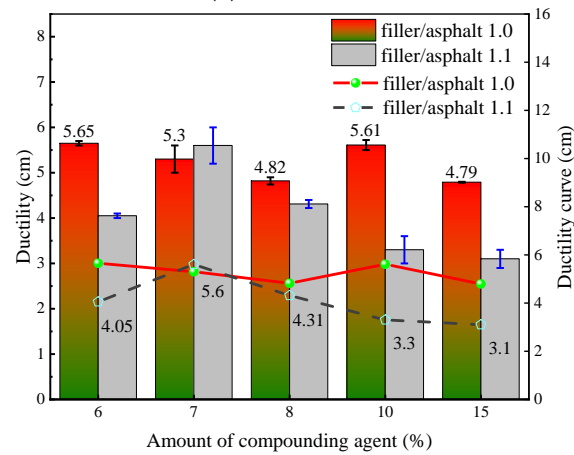
### 4.1. Asphalt Mastic

#### 4.1.1. Conventional Performance

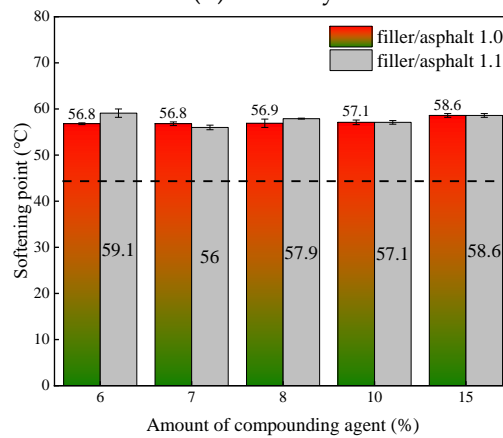
The asphalt mastic with different amounts of flame retardant and smoke suppressant compound was tested for conventional performance, including penetration ductility and softening point. In this way, the basic properties of this material were studied, and the results are shown in Figure 6.



(a) Penetration



(b) Ductility



(c) Softening point

**Figure 6.** Conventional performance of flame retardant asphalt mastic with different filler/asphalt: (a) penetration, (b) ductility, and (c) softening point.

In Figure 6a, the penetration of these two asphalt mixtures with different fillers/asphalt showed an increasing, and then decreasing trend. The maximum flame retardant was found at 7% with different filler/asphalt ratios. The standard deviations of penetration for the two different filler/asphalt ratios were 7.3 and 2.9, respectively. The penetration dispersion degree of asphalt mastic with filler/asphalt ratio of 1.1 was reduced by 55% compared with that of filler/asphalt of 1.0 under different dosing of flame retardant. Figure 6b shows that the maximum ductility for both filler/asphalt ratios was about 5.6 cm. However, when the filler/asphalt ratio was less than 1.1, the ductility showed the law of increasing and then decreasing with the increase of flame retardant, and the change was not obvious at the filler/asphalt ratio of 1.0. Figure 6c shows that the softening points for different filler/asphalt ratios were 24% higher than the standard values for virgin asphalt. However, the lowest softening point was found at 7% flame retardant addition. At a filler/asphalt ratio of 1.1, the softening point showed a trend of decreasing, and then increasing with the increase of flame retardant dosage. However, this trend was not obvious in the case of filler/asphalt ratio of 1.0.

It should be noted that the asphalt mastic formed by adding mineral powder and fire retardant to asphalt was used in this test. Accordingly, the overall penetration compared with 90# virgin asphalt, the value decreased to more than 50%. The reason for this is that the virgin asphalt hardens with the addition of mineral powder. For both filler/asphalt ratios, the difference in penetration was the largest at 6% flame retardant dosage, with a difference of about 33%. It was also found that the difference in penetration at these two filler/asphalt ratios gradually decreased with the increase in the content of flame retardant and smoke suppressant. It also showed that mineral dust hardens virgin asphalt; by the same principle, the plasticity of the virgin asphalt after the addition of mineral powder was reduced in the ductility test. The maximum value of ductility was about 5.6 cm. Unlike the above, the softening point had little effect, and to some extent was slightly increased.

In the case of filler/asphalt ratio of 1.1, the general trend of permeability, ductility, and softening point: the permeability and ductility increased and then decreased with the increase of flame retardant dosage, and the softening point decreased and then increased with the increase of flame retardant dosage. The inflection point in the above analysis occurs at 7% flame retardant dosage. Therefore, the dosage of flame retardant smoke suppressant was determined to be 7%.

#### 4.1.2. Low-Temperature Rheological Properties

The low-temperature rheological properties were tested by BBR to simulate the mechanical response of asphalt under pavement temperature stress. Creep stiffness modulus  $s$  and creep rate  $m$  were derived for evaluating the deformation resistance and low-temperature relaxation properties of asphalt materials, respectively. The creep stiffness modulus  $s$  and creep rate  $m$  at 60 s were chosen for the tests at  $-6\text{ }^{\circ}\text{C}$ ,  $-12\text{ }^{\circ}\text{C}$ , and  $-18\text{ }^{\circ}\text{C}$ . The results are shown in Figure 7.

Cracks occurred in asphalt pavements in low-temperature environments due to the inadequate low-temperature crack resistance of asphalt [38]. The low-temperature rheological properties of asphalt mastic with two kinds of flame retardant and smoke suppressant compounds were studied, and the creep stiffness  $s$  and creep rate  $m$  values are shown in Figure 7. Creep stiffness  $s$  can evaluate the temperature shrinkage of asphalt materials; a greater creep stiffness indicates a higher temperature stress, resulting in a greater likelihood of cracking. The  $m$  value can characterize the rate of change of the creep stiffness of asphalt materials under low-temperature conditions; a greater value of  $m$  indicates that the material has a higher ability to relax stresses [39]. According to the superior performing asphalt pavement (abbreviated as "Superpave"), in order to ensure the low-temperature performance of asphalt, it is necessary to ensure that  $s \leq 300\text{ MPa}$  and  $m \geq 0.30$ . Firstly, in Figure 7a, stiffness modulus of asphalt mastic with two different blends showed an increasing trend with a decrease of temperature. However, 7% content of flame retardant and smoke suppression compound asphalt mastic at  $-6\text{ }^{\circ}\text{C}$  and  $-12\text{ }^{\circ}\text{C}$  did not reach the

upper limit of 300 MPa; its low-temperature performance was significantly better than 0% content of asphalt mastic. From the creep rate index analysis in Figure 7b, the creep rates of the two different blends of asphalt mastic showed a decrease with temperature. Further analysis revealed that the  $m$ -value of the asphalt mastic with 7% fire retardant and smoke suppressant compounds complied with the lower limit at  $-6\text{ }^{\circ}\text{C}$ ,  $-12\text{ }^{\circ}\text{C}$ , and  $-18\text{ }^{\circ}\text{C}$ , while the  $m$ -value at  $-12\text{ }^{\circ}\text{C}$  exceeded the lower limit by 30%. It fully illustrates that the asphalt mastic containing 7% flame retardant inhibitor compound has superior low-temperature rheology. Fire retardant and smoke suppressant can not only achieve the effect of fire retardant and smoke suppressant, but also improve the low-temperature performance of asphalt mastic.

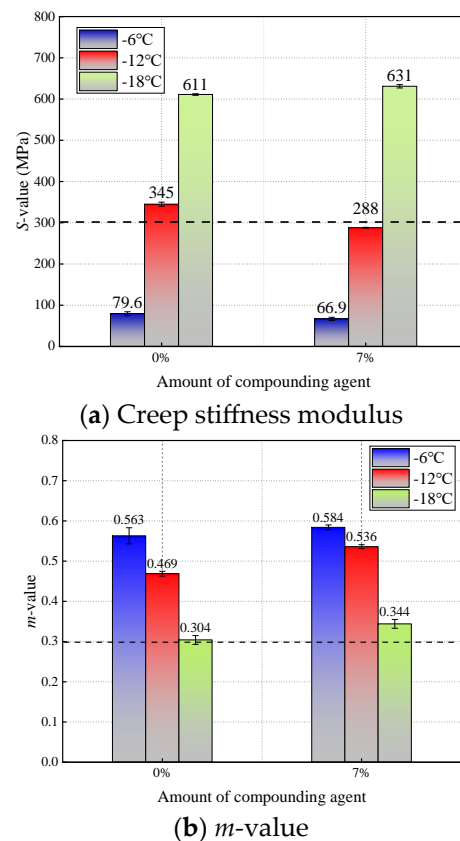


**Figure 7.** Different flame retardant and smoke suppressing compound doses of asphalt mastic BBR test: (a) creep stiffness modulus, (b)  $m$ -value.

The  $S$  value at the three temperatures did not differ by more than 20% for two different flame retardant and smoke suppressant dosages (0%, 7%). At 7% fire retardant and smoke suppressant dosage of asphalt mastic, its low-temperature performance was better than other dosages of asphalt mastic. However, at  $-18\text{ }^{\circ}\text{C}$ , the  $S$  value (611, 631) did not differ much, which to some extent reflects that the low-temperature performance of asphalt mastic had little relationship with the dosage of fire retardant and smoke suppressant.

#### 4.1.3. High-Temperature Rheological Properties

Temperature sweep tests were used to evaluate the high-temperature rheological properties of asphalt, whereas in this study,  $G^*/\sin\delta$  was used to characterize the high-temperature resistance to permanent deformation of asphalt mastic. The results are shown in Figure 8. The frequency sweep test was also used to characterize the rheological properties of the asphalt material. Using the time–temperature superposition principle, the viscoelastic parameters at different temperatures were transformed into the viscoelastic parameters at the base temperature of  $28\text{ }^{\circ}\text{C}$ . Thus, the master curves of the asphalt material

were obtained, and the low-frequency (high-temperature) part was chosen to be analyzed in this study. The results are shown in Figure 8.

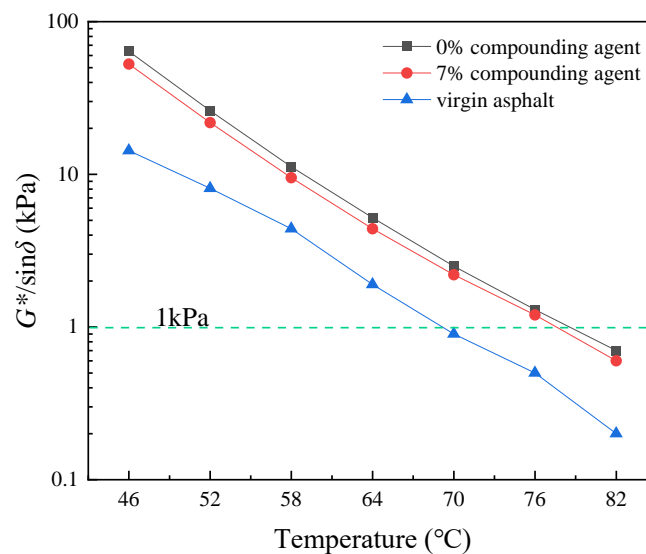


**Figure 8.**  $G^*/\sin\delta$  for different asphalt mastics.

In Figure 8, the rutting factor ( $G^*/\sin\delta$ ) in the Superpave system was used to evaluate the high-temperature resistance of asphalt to permanent deformation. It represents the modulus of energy dissipation during creep. At the same temperature, the value of  $G^*/\sin\delta$  becomes larger, which indicates that the energy dissipation value becomes smaller, flow deformation becomes smaller, and rutting resistance becomes stronger, which proves that high-temperature performance improves [40]. Firstly,  $G^*/\sin\delta$  showed a good linear correlation with temperature in semi-log-temperature coordinates. The rutting factor of the asphalt mastic was greatly improved by the addition of mineral powder, which enhanced the rutting resistance of the asphalt mastic. However, the rutting factor was reduced with the addition of 7% flame retardant and smoke suppressant. Between 70 and 82 °C, the rutting resistance of the 7% fire retardant and smoke retardant asphalt mastics was close to that of the 0% fire retardant and smoke retardant asphalt mastics. The critical temperature was the lowest temperature corresponding to  $G^*/\sin\delta \geq 1.0$  kPa. In terms of critical temperature, the critical temperature of asphalt mastic containing 7% flame retardant and smoke suppressant was 77 °C. The difference between the critical temperatures of asphalt mastic with 7% fire retardant content and asphalt mastic with 0% fire retardant was 2 °C, which was not significant.

From Figure 8, the high-temperature critical temperature of asphalt mastic with 7% flame retardant and smoke suppressant compound was 77 °C, which exceeded the high-temperature critical temperature of the original asphalt by 10%. The increase in critical temperature compared to virgin asphalt somewhat showed that the fire retardant and smoke suppressant improved the high-temperature performance of the asphalt mastic.

In Figure 9, in the same frequency range, in phase I, although the two asphalt mastics had approximately the same magnitude of change in complex shear modulus, in a certain sense they had lower temperature sensitivity. However, in the low-frequency (I, II) zone, the asphalt mastic mixed with 7% flame retardant smoke suppressant compound had the largest complex shear modulus, so it had better high-temperature performance. The same conclusions from the high-temperature rheological performance and low-temperature rheological performance study were obtained.

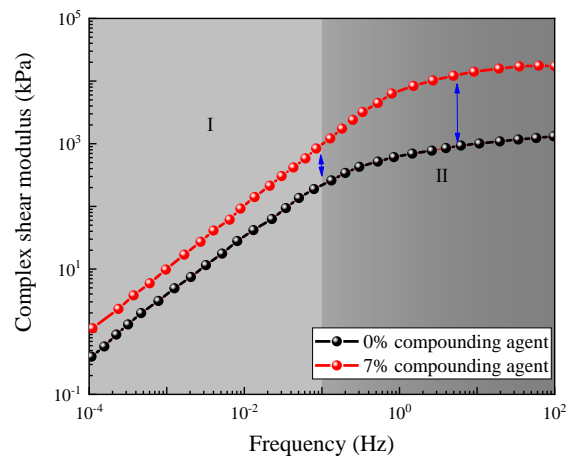
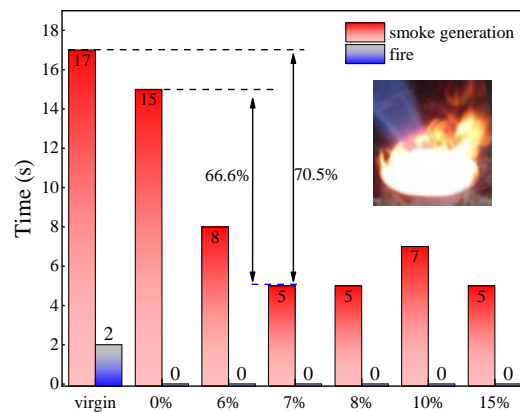


**Figure 9.** Master curves of low-frequency complex shear modulus for different types of asphalt.

#### 4.2. Analysis of Flame Retardant and Smoke Suppression Effect of Asphalt Mastic

##### 4.2.1. Indoor Combustion and Cone Calorimetry Analysis

Through the smoke generation time and smoke area, the flame retardant smoke suppression performance of asphalt mastic was evaluated, and the results are shown in Figures 10 and 11. The dosage of flame retardant and smoke suppressant with significant effect was determined based on the indoor combustion test. Then, a conical calorimeter was used for precise analysis, and the results are shown in Figure 10.



Virgin asphalt and asphalt mastic with different compound dosing

**Figure 10.** Indoor combustion effect.

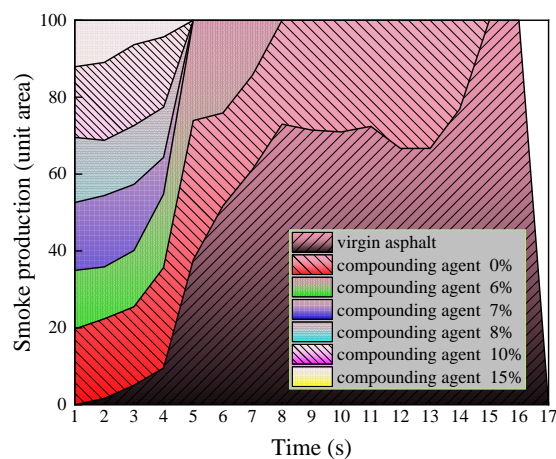


**Figure 11.** Smoke-generating area of asphalt mastic with different amounts of compounding agents.

In Figures 10 and 11, the fire retardant effect of the asphalt mastic mixed with the compound can be observed after 10 s from ignition. The virgin asphalt had about 2 s of open flame burning, which was not seen in other test groups. By comparing the burning area at intermediate moments, it was found that the burning time tended to shorten as the amount of flame retardant and smoke suppressant increased. The smoke duration of the flame retardant and smoke suppressant (6%, 7%, 8%, 10%, 15%) was less than 10 s, which showed the obvious effect of flame retardant and smoke suppressant. Notably, in Figure 10, the amount of smoke doped with 10% fire retardant smoke suppressant is higher than the neighboring group, which is considered to be generated by the stability of the asphalt mastic in the test. Overall, it does not affect the trend of the effect of flame retardant smoke suppression with flame retardant doping. The presence or absence of flames from the virgin asphalt and other controls side-steps the fact that the mineral powders also produced some fire retardant effects. In terms of smoke generation time, the asphalt mastic with 7% fire retardant and smoke suppressant shortened the smoke generation time by 70.5% and 66.6% compared with virgin asphalt and asphalt mastic with 0% fire retardant and smoke suppressant, respectively. The flame retardant and smoke suppressant effect of the flame retardant and smoke suppressant was fully demonstrated, and 7% was found to be the optimal dosage.

Through comprehensive analysis, the dosage of flame retardant and smoke suppressant was confirmed to be 7%. In particular, the determination of the mineral powder category used in this subsection was determined in the Marshall flow value stability test.

The specimens of 0% and 7% of two flame retardant and smoke suppressant compound doping were tested by the conical calorimeter, as shown in Figure 12. The smoke rate of the test showed that the smoke moment of the asphalt mastic without flame retardant and smoke suppressant was at least 20 s earlier than that of the asphalt mastic with 7% flame retardant and smoke suppressant, and the extinguishing time was at least 25 s later.

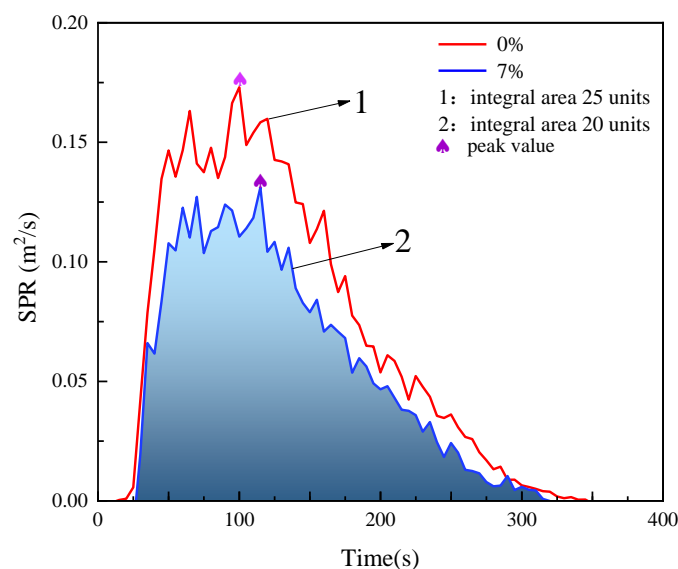


**Figure 12.** Conical calorimetric–smoke generation rate diagram.

The difference in peak smoke emission between the sample without flame retardant and smoke suppressant and the sample with 7% flame retardant and smoke suppressant was more than 40%. It showed that the flame retardant smoke suppression effect of compounding agent with 7% was obvious. From the point of view of smoke integral area: after mathematical integration, the integral area of the unadulterated composite sample was 25 units; the integral area of the 7% flame retardant and smoke suppressant addition was 20 units. The amount of smoke was reduced by 20%. In contrast, asphalt mastic with

7% flame retardant and smoke suppressant achieved a significant flame retardant and smoke suppressant effect.

#### 4.2.2. Thermogravimetric Analysis of Flame Retardant Asphalt Mastic

The TG tests were conducted at high temperatures for asphalt mastics. The amounts of flame retardant and smoke suppressant were 0% and 7%, respectively. The pyrolysis temperature and mass changes of asphalt mastic were obtained under different temperature change conditions. Tests were conducted to characterize the flame retardant effect of fire retardant and smoke suppressants in asphalt. The results are shown in Figure 13.

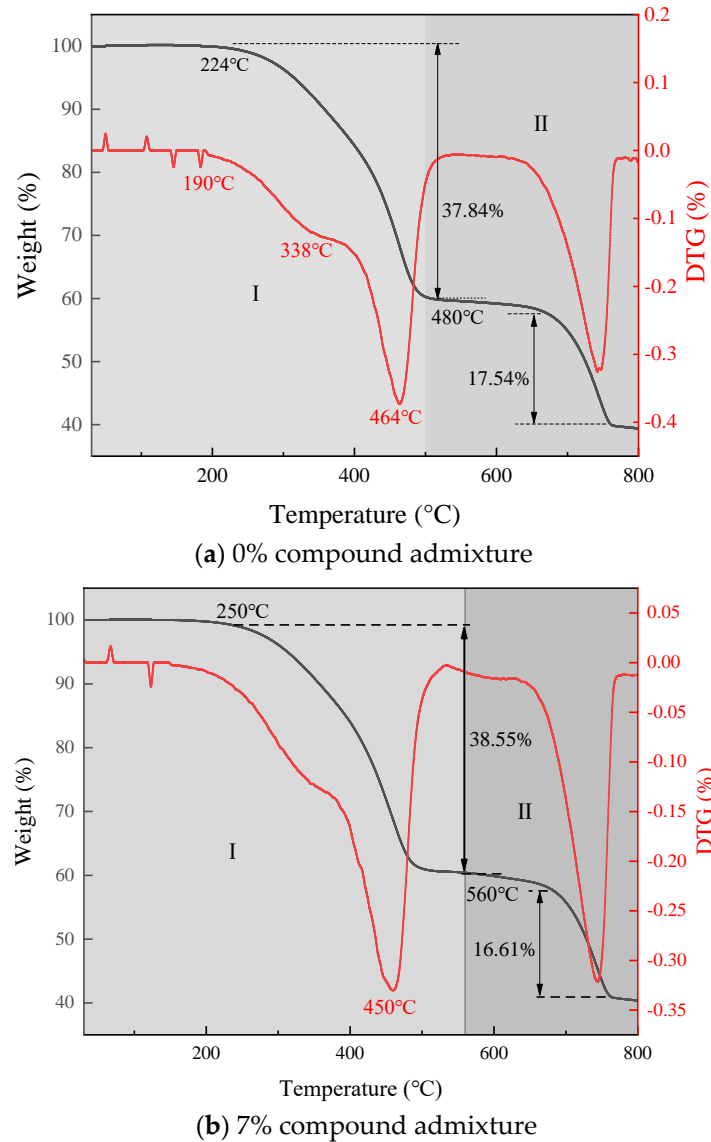


**Figure 13.** TG analysis graph: (a) 0% compound admixture, (b) 7% compound admixture.

In the TG analysis, it was found that the fire retardant asphalt mastic was basically divided into two pyrolysis segments, which developed in a roughly cyclical manner (part I and II), with part I being the most dominant pyrolysis stage. Meanwhile, for 7% flame retardant compared to 0% flame retardant and smoke suppressant asphalt mastic, the thermal decomposition temperature increased by 25 °C at the beginning of the first stage and 80 °C at the end of the first stage, and the mass loss in the first stage was about 38%. It can be seen that the flame retardant and smoke suppressant has a significant flame retardant effect in asphalt mastic. From the conductivity thermogravimetric analysis curve,

the asphalt mastic mixed with 7% compound started to absorb heat after 250 °C. The flame retardant and smoke suppressant delays the volatilization of the burning material of the asphalt mastic, and the magnesium oxide produced by pyrolysis promotes the rapid dehydration and carbonization of the polymer surface [41], forming a carbonized layer, which achieves the flame retardant effect. The maximum flame retardant effect was achieved at about 450 °C. Comparing the residual amount of fire retardant asphalt mastic at the two dosages, the residual amount of fire retardant asphalt mastic at a dosage of 7% remained above 40% in the TG analysis.

#### 4.2.3. Microscopic Analysis of Asphalt Mastic

The specimens were taken for flame burning (about 300 °C) and TG test (about 800 °C). The surfaces were observed by SEM to study the state of the asphalt [42].

The surface of asphalt mastic doped with flame retardant and smoke suppressant compound was analyzed by SEM on the reaction surface at two temperatures (ordinary flame temperature at about 300 °C, and the highest temperature of TG test at about 800 °C).

In Figure 14a, the asphalt layer adhering to the mineral powder surface first contacted with the flame, and the asphalt on the surface was pyrolytically evaporated (the surface of the mineral powder was exposed) without flame retardant and smoke suppressant effect. On the contrary, in Figure 13b, the asphalt layer adhering to the surface of the mineral powder does not evaporate thermally in the presence of the flame retardant and smoke suppressant (the mineral powder is wrapped by the asphalt). SEM observation at flame burning temperature (approx. 300 °C) showed that asphalt pastes containing 7% flame retardant and smoke suppressant has a significant flame retardant and smoke suppressant effect after flame burning.

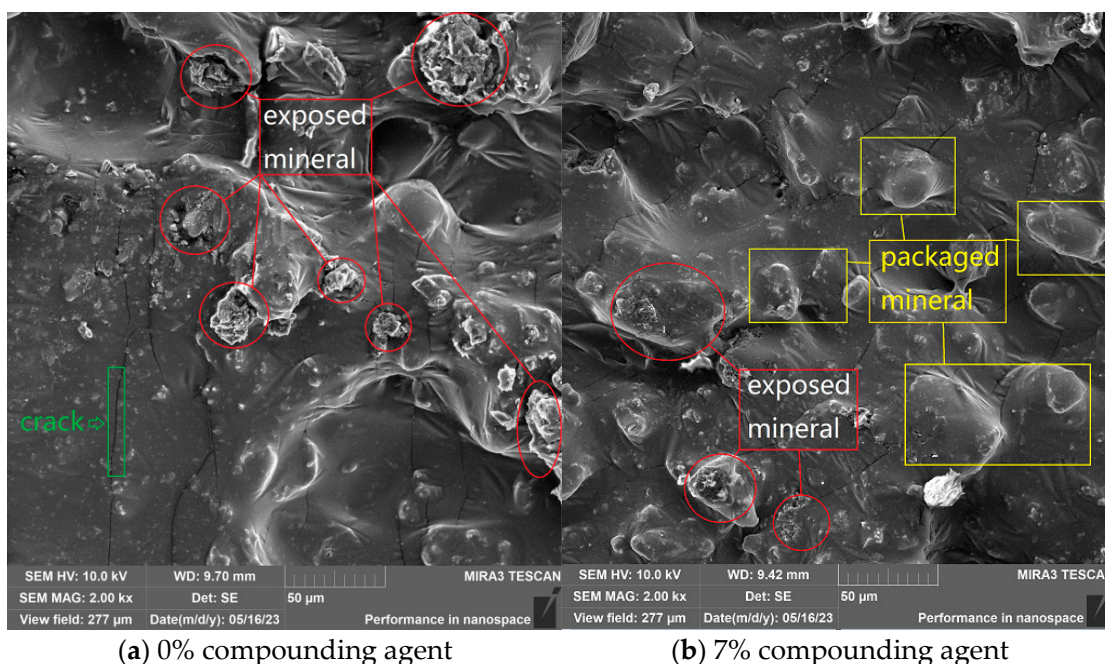


**Figure 14.** SEM microscopic images after flame burning (about 300 °C): (a) 0% compounding agent, (b) 7% compounding agent.

Figure 15 shows the surface of the residual specimen after the TG test. In Figure 15a, the asphalt bonded to the surface of the mineral powder was completely pyrolytically volatilized (lamellar lattices appear). The surface of the mineral powder showed distinct angularity, and the asphalt around the mineral powder showed pyrolytic deficiency. In Figure 14b, the surface of the asphalt mastic showed pyrolytic softening, with some particles on the surface showing pyrolysis (small amounts of lattice bodies). However, most of the

asphalt mastic adhering to the surface of the mineral powder did not pyrolyze. In contrast, in Figure 15a, it was found that the asphalt on the surface of the mineral powder was pyrolyzed and appeared as a laminated lattice. The reason is that the mineral powders are joined together in the form of flaky particles after being subjected to a high temperature of 800 °C. Due to the distortion of the lattice during calcination, there is an increase in aggregates as hydroxyl groups are removed. In contrast, asphalt with 7% flame retardant and smoke suppressant did not show similar phenomena. Thus, the change in the surface state of the asphalt proves the important role and applicability of fire retardant inhibitors.

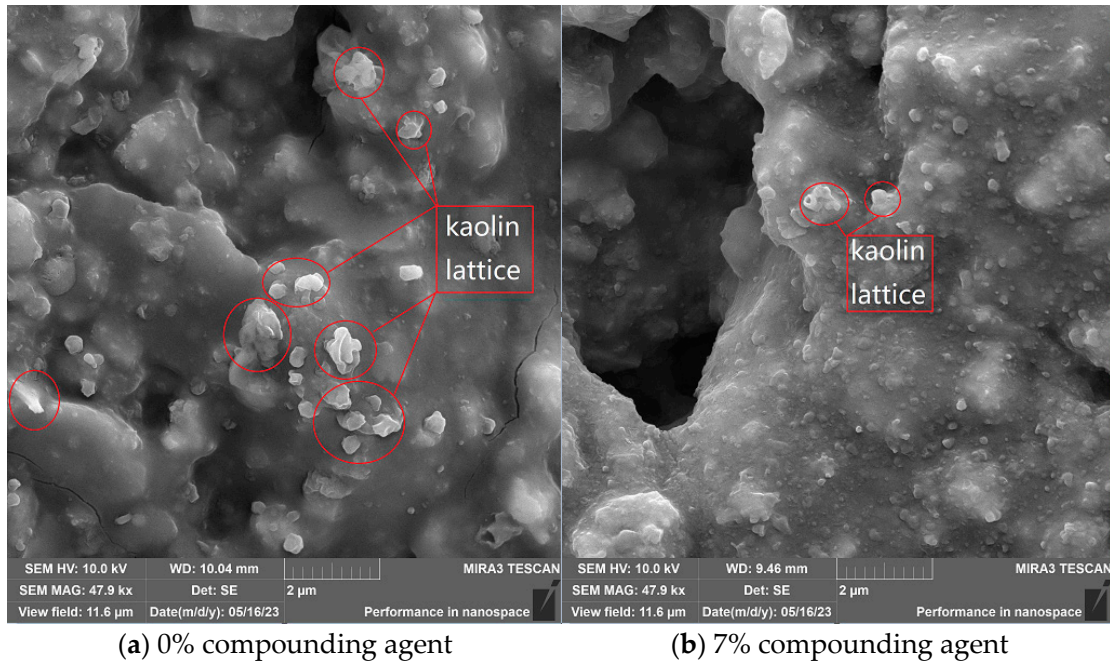


**Figure 15.** SEM microscopic images of the samples tested by TG (about 800 °C): (a) 0% compounding agent, (b) 7% compounding agent.

#### 4.3. Analysis of Performance of Asphalt Mixtures

##### 4.3.1. Flow Value and Stability of Asphalt

The optimal type of mineral powder (as one of the three mineral powders from the Dalian area) was determined by stability and flow value. The results are shown in Figure 16.

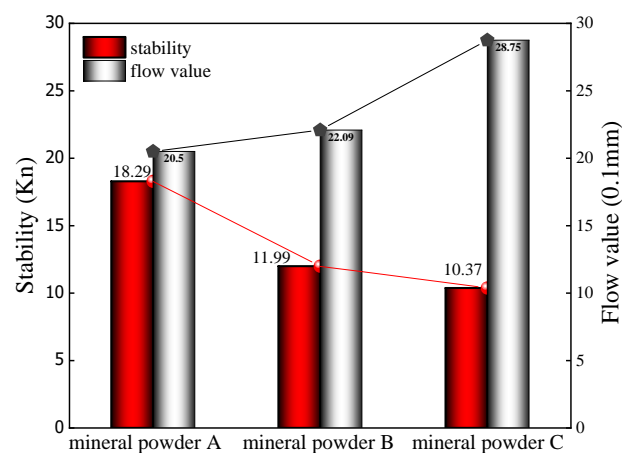


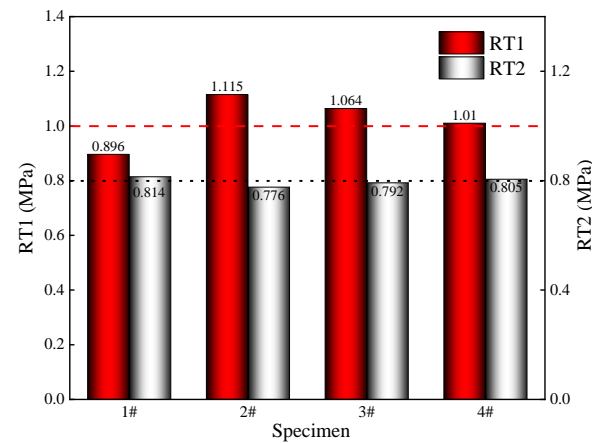
**Figure 16.** Comparison of Marshall stability and flow value of different mineral powders.

In Figure 16, the specimen with A mineral powder showed a maximum value of 18.29 kN of stability, and also a minimum value (2.05 mm) of flow. The stability and small

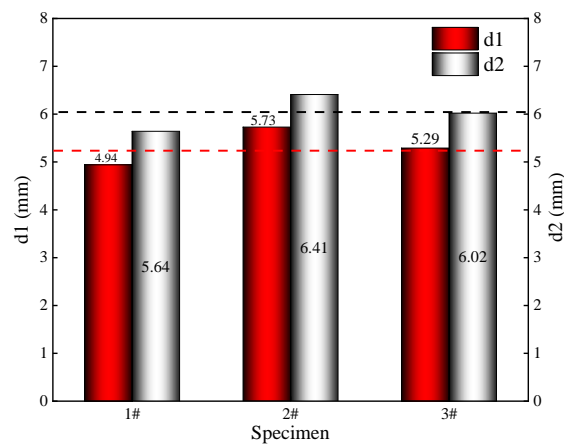
deformation were good, indicating that the asphalt mixture strength was higher. Therefore, A mineral powder was selected for the subsequent index test.

#### 4.3.2. Asphalt Mixture Performance Analysis

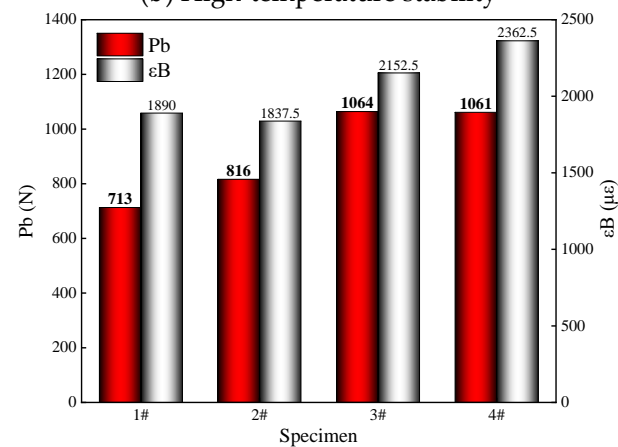
On the basis of research on fire retardant asphalt mastics, the effect of flame retardant and smoke suppressant compound on asphalt mixture performance was further investigated. The results are shown in Figure 17.



(a) Water stability



(b) High-temperature stability



(c) Low-temperature stability

**Figure 17.** Performance of asphalt mixtures: (a) water stability, (b) high-temperature stability, and (c) low-temperature stability.

In Figure 17a, the water stability of fire retardant asphalt mixtures (7%) was investigated in asphalt mixture performance tests. The freeze–thaw split test was used, and the calculated freeze–thaw split strength ratio was 78%, which exceeded the standard value by 4%. In Figure 17b, the dynamic stability of the rutting plate calculated in the high-temperature stability test was 896 (number of times/mm), which exceeded the standard value by more than 12%. The coefficient of variation was 3.5%, which met the requirements of asphalt pavement. In Figure 17c, the maximum bending tensile strain calculated in the low-temperature stability ( $\mu\epsilon$ ) experiments was 2060, which exceeded the standard value of winter temperature zone and winter cold zone by 3%. The addition of such flame retardant asphalt mixture fully meeting the asphalt mixture performance should be verified by experiments, more from the perspective of practicality.

#### 4.4. Flame Retardant and Smoke Suppression Analysis of Asphalt Mixture

Indoor laboratory combustion tests were conducted on Marshall specimens containing different dosages of flame retardant and smoke suppressant (0%, 7%). The mass loss of each group was recorded at an interval of 30 s to analyze the flame retardant and smoke suppression performance of asphalt mixture with two different amounts of flame retardant compound. The weight loss variations were analyzed, as shown in Figure 18.

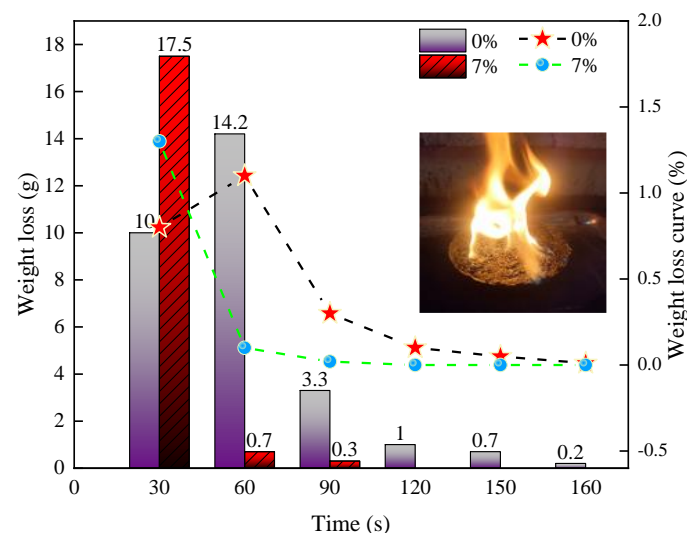


Figure 18. Specimen burning weight loss.

In Figure 18, in terms of weight loss, the burning time of specimens containing 7% flame retardant smoke suppressant was up to 90 s. At the 30 s timepoint, although the weight loss of the asphalt mixture containing 7% flame retardant and smoke suppressant was maximized, the burning time was reduced by 43% compared to the asphalt mixture without flame retardant and smoke suppressant. In addition, the total weight loss of the specimen with 7% flame retardant was 37% less than that of the specimen with 0% flame retardant during the whole combustion process.

From the analysis of weight loss rate, in 30–60 s, although the weight loss rate of 7% flame retardant and smoke suppressant specimen was the largest, after 60 s, there was basically no significant change in the weight loss rate. This means that the flame retardant and smoke suppression effect is enacted quickly in the shortest time. On the contrary, the weight loss of specimens with 0% flame retardant and smoke suppressant showed a pattern of increasing and then decreasing, and the weight loss of burning time over 1 g lasted until 120 s. Through the above analysis, asphalt mixtures containing fire retardant and smoke suppressant have significant fire retardant and smoke suppressant effects.

## 5. Conclusions

This article focused on solving the problem of flame retardant and smoke suppression of asphalt mixtures, which largely reduced the hazards of asphalt fumes on construction workers and the environment, while meeting the requirements of pavement use. The application of flame retardant and smoke suppressant with magnesium hydroxide as the main component in asphalt materials was fully verified. In this article, the mechanical properties of flame retardant asphalt mastic were investigated by using BBR and DSR, and the flame retardant and smoke inhibition properties of flame retardant asphalt mastic were investigated by using SPR and TG. For fire retardant asphalt mixtures, the low-temperature splitting test, high-temperature rutting test, and combustion test were used to investigate the roadworthiness and combustion properties.

This article drew the following conclusions:

- The asphalt mastic doped with fire retardant and smoke suppressant improved the low-temperature rheology and reduced the high-temperature rheology to varying degrees. Fire retardant and smoke suppressant asphalt mastic had excellent low-temperature rheological properties.
- Asphalt mastic and asphalt mixtures containing 7% fire retardant and smoke suppressant had the best fire retardant and smoke suppressant effect.
- Asphalt mixtures containing fire retardant and smoke suppressant had reliable water stability, high-temperature performance, and low-temperature tensile properties for asphalt pavement in Chinese tunnels.
- The pyrolysis initiation and termination temperatures of the asphalt mastic containing fire retardant and smoke suppressant were substantially increased during the main combustion phase (I).
- After burning at 800 °C, a small amount of pyrolysis occurred in the asphalt layer containing fire retardant and smoke suppressant. The flame retardant effect is obvious.
- Burning time, smoke emission time, and weight loss of asphalt mixtures containing fire retardant and smoke suppressant were significantly reduced.

In this article, the combustion properties and pavement material properties of fire retardant asphalt mastic and fire retardant asphalt mixtures were investigated by multiscale test methods, respectively. The above conclusions were obtained. The asphalt mixture containing magnesium hydroxide reduced the volatilization of asphalt smoke to a greater extent, which protected the environment and personal health, and at the same time, ensured the quality of construction workers in tunnel construction.

There are some limitations in this article, and no kinetic aspects of fire retardant asphalt mastic have been investigated. In-depth research in this area can be strengthened in the next research work.

**Author Contributions:** J.L.: conceptualization, methodology, writing—original draft, software, data curation; M.H.: supervision, visualization; C.Z.: supervision, visualization, funding acquisition, writing—review and editing; F.L.: visualization, writing—review and editing, software; L.S.: writing—review and editing, data curation; P.C.: supervision, investigation. All authors have read and agreed to the published version of the manuscript.

**Funding:** This investigation were supported by Fundamental Research Funds for the Central Universities ,Grant Nos. DUT20JC50 and DUT17RC (3)006; and the National Natural Science Foundation of China, Grant No. 51508137.

**Data Availability Statement:** Some or all of the data or code supporting the results of this study are available from the corresponding authors upon request.

**Acknowledgments:** The authors are grateful for the above grants; We are grateful to journal workers and reviewers for their support.

**Conflicts of Interest:** The authors declare no conflict of interest.

## Abbreviations

BBR	bending beam rheometer
DSR	dynamic shear rheological
TG	thermogravimetric
DTG	derivative thermogravimetry
SEM	scanning electron microscopy
SBS	styrene-butadiene-styrene
FH	fire hardness
XRD	X-ray diffraction
XRF	X-ray fluorescence
SPR	smoke production rate

## References

- Tang, L.; Zhang, X.; Wang, C.W.; Lang, A.C.; Wang, Y.G.; Wang, C.L.; Zhao, P.H. Study on performance of tunnel warm-mixed flame retardant asphalt mixture. *China Water Transp.* **2023**, *23*, 137–139+142.
- Li, Q.R.; Xu, X.Q.; Jia, Z.Y.; Chen, X.B. Flame retardant and road performance of ABA-Ti composite flame retardant asphalt. *J. Wuhan Univ. Technol.* **2021**, *45*, 971–975.
- Wang, L.D. *Research on the Performance of Environmentally Friendly Smoke-Suppressing Asphalt and Its Mixes*; Chongqing Jiaotong University: Chongqing, China, 2013.
- Ren, F.; Zhang, X.J.; Sun, H.B.; Chen, J.F.; Zhang, L.Q. Current status and prospects of flame retardant asphalt for roads at home and abroad. *J. Chang. Univ.* **2012**, *32*, 1–10.
- Yang, X.; Shen, A.; Jiang, Y.; Meng, Y.; Wu, H. Properties and mechanism of flame retardance and smoke suppression in asphalt binder containing organic montmorillonite. *Constr. Build. Mater.* **2021**, *302*, 124148. [[CrossRef](#)]
- Liu, X.P.; Xi, W.B.; Zou, Y.X.; Jiang, Q.; Wu, S.P. Effect of flame retardant warm mix compound modification on the high and low temperature performance of asphalt. *J. Wuhan Univ. Technol.* **2022**, *46*, 532–536.
- Li, X.; Zhou, Z.; Deng, X.; You, Z. Flame Resistance of Asphalt Mixtures with Flame Retardants through a Comprehensive Testing Program. *J. Mater. Civ. Eng.* **2017**, *29*, 04016266. [[CrossRef](#)]
- Liu, D.L.; Yan, Y.Z.; Huang, Y.Y.; Yao, J.L.; Yuan, J.B. Study on flame-retardant properties of flame retardant asphalt mixture. In *Applied Mechanics and Materials*; Trans Tech Publications Ltd.: Bäch, Switzerland, 2013; Volume 438, pp. 387–390.
- Qiu, J.; Yang, T.; Wang, X.; Wang, L.; Zhang, G. Review of the flame retardancy on highway tunnel asphalt pavement. *Constr. Build. Mater.* **2019**, *195*, 468–482. [[CrossRef](#)]
- Yuan, Y.Q.; Wang, X.S.; Guo, T. Study on Warm Mix Flame Retardant Asphalt Mixture. In *Applied Mechanics and Materials*; Trans Tech Publications Ltd.: Bäch, Switzerland, 2013; Volume 438, pp. 395–398.
- Li, B.; Wen, Y.; Li, X. Laboratory Evaluation of Pavement Performance and Burning Behavior of Flame-Retardant Asphalt Mixtures. *J. Test. Eval.* **2016**, *45*, 20160029. [[CrossRef](#)]
- Qin, X.; Zhu, S.; Chen, S.; Li, Z.; Dou, H. Flame retardancy of asphalt mixtures and mortars containing composite flam-retardant materials. *Road Mater. Pavement Des.* **2014**, *15*, 66–77. [[CrossRef](#)]
- Wu, Q.; Lü, J.; Qu, B. Preparation and characterization of microcapsulated red phosphorus and its flame-retardant mechanism in halogen-free flame retardant polyolefins. *Polym. Int.* **2003**, *52*, 1326–1331. [[CrossRef](#)]
- Wang, H.J.; Chen, L.X.; Miao, H. Research and application overview of nitrogen-based flame retardants. *Thermosetting Resins* **2005**, *20*, 36–41.
- Liang, Y.S. *Preparation of Aluminum Hydroxide/Layered Silicate Flame Retardant Asphalt and Its Synergistic Flame Retardant Mechanism*; Wuhan University of Technology: Wuhan, China, 2013.
- Hu, S.G. Research on alkaline filler flame-retarded asphalt pavement. *J. Wuhan Univ. Technol. Mater. Sci. Engl. Ed.* **2006**, *21*, 146–148.
- Qin, X.; Zhu, S.; Li, Z.; Chen, S. Dynamic mechanical characterizations and road performances of flame retardant asphalt mortars and concretes. *J. Wuhan Univ. Technol. Sci. Ed.* **2015**, *30*, 1036–1042. [[CrossRef](#)]
- Li, Y.; Liu, S.; Xue, Z.; Cao, W. Experimental research on combined effects of flame retardant and warm mixture asphalt additive on asphalt binders and bituminous mixtures. *Constr. Build. Mater.* **2014**, *54*, 533–540. [[CrossRef](#)]
- Cong, P.; Yu, J.; Wu, S.; Luo, X. Laboratory investigation of the properties of asphalt and its mixtures modified with flame retardant. *Constr. Build. Mater.* **2008**, *22*, 1037–1042. [[CrossRef](#)]
- Tan, Y.; Xie, J.; Wu, Y.; Wang, Z.; He, Z. Performance and Microstructure Characterizations of Halloysite Nanotubes Composite Flame Retardant-Modified Asphalt. *J. Mater. Civ. Eng.* **2023**, *35*, 04022448. [[CrossRef](#)]
- Zhou, Y.; Liu, T.; Zhang, G.; Du, L.; Zhang, Y.; Jing, H.; Lu, M. Study on microstructure and flame retardant performance of tunnel flame retardant asphalt. *Appl. Chem. Ind.* **2023**, *52*, 2353–2357+2361.
- Lin, Y.; Liu, S.; Huang, H.; Shi, W.; Li, M. High and low-temperature performance of warm-mixed flame retardant asphalt based on rheological characteristics. *J. Jiangsu Univ.* **2023**, *44*, 483–489.

23. Jianying, Y.; Peiliang, C.; Shaopeng, W. Investigation of the properties of asphalt and its mixtures containing flame retardant modifier. *Constr. Build. Mater.* **2009**, *23*, 2277–2282. [[CrossRef](#)]
24. Bonati, A.; Merusi, F.; Bochicchio, G.; Tessadri, B.; Polacco, G.; Filippi, S.; Giuliani, F. Effect of nanoclay and conventional flame retardants on asphalt mixtures fire reaction. *Constr. Build. Mater.* **2013**, *47*, 990–1000. [[CrossRef](#)]
25. Zhu, K.; Wang, Y.; Tang, D.; Wang, Q.; Li, H.; Huang, Y.; Huang, Z.; Wu, K. Flame-Retardant Mechanism of Layered Double Hydroxides in Asphalt Binder. *Materials* **2019**, *12*, 801. [[CrossRef](#)] [[PubMed](#)]
26. Sheng, Y.; Wu, Y.; Yan, Y.; Jia, H.; Qiao, Y.; Underwood, B.S.; Niu, D.; Kim, Y.R. Development of environmentally friendly flame retardant to achieve low flammability for asphalt binder used in tunnel pavements. *J. Clean. Prod.* **2020**, *257*, 120487. [[CrossRef](#)]
27. Xu, T.; Huang, X.; Zhao, Y. Investigation into the properties of asphalt mixtures containing magnesium hydroxide flame retardant. *Fire Saf. J.* **2011**, *46*, 330–334. [[CrossRef](#)]
28. Xia, W.; Zhou, X.; Yang, X. Suppressive effects of composite flame retardant on smoke release, combustion soot and residue constituents of asphalt mixture. *J. Energy Inst.* **2022**, *103*, 60–71. [[CrossRef](#)]
29. Haojia, J.; Yadong, H.; Ke, W.; Kai, Z. Influence of aging on the performance and flame retardant properties of inorganic compound flame retardant asphalt for road use. *Fire Sci. Technol.* **2023**, *42*, 747–751.
30. Wei, X. Study on the application of flame retardant asphalt mixture in tunnel pavement. *Heilongjiang Commun. Sci. Technol.* **2023**, *46*, 109–111.
31. Lu, J.; Du, A.; Liu, W.; Sun, C. Study on flame retardant effect of two asphalt pavement flame retardants. *Nonferrous Met. Mater. Eng.* **2023**, *44*, 75–84.
32. Wang, X.; Xu, J.; Mub, Z. Study on the X-ray diffraction physical phase analysis method of crystals. *Exp. Technol. Manag.* **2021**, *38*, 29–33. [[CrossRef](#)]
33. Huang, Q.Q.; He, R.; Chen, H.X. Effect of powder to rubber ratio on the performance of AC-16 asphalt mixes. *Chin. Sci. Tech. Pap.* **2019**, *14*, 1289–1293.
34. Huang, Y.D.; Lin, C.H.; Jiang, H.J.; Wu, K.; Zhu, K. Effect of aluminum hydroxide flame retardant particle size on asphalt properties. *Fire Sci. Technol.* **2021**, *40*, 1068–1071.
35. Hu, K.; Li, M.L. Study on the rheological and flame retardant properties of magnesium hydroxide on asphalt. *Transp. Sci. Technol.* **2020**, 106–109.
36. Liu, F.; Pan, B.; Bian, J.; Zhou, C. Experimental investigation on the performance of the asphalt mixture with ceramic fiber. *J. Clean. Prod.* **2023**, *384*, 135585. [[CrossRef](#)]
37. Li, H.; Zou, X.L.; Chen, C.Y. Study on flame retardant and smoke suppression properties of flame retardant asphalt mixtures and road use performance. *J. Build. Mater.* **2012**, *15*, 6. [[CrossRef](#)]
38. Shen, J.N. *Road Performance of Asphalt and Asphalt Mixtures*; People's Traffic Publishing House: Beijing, China, 2009; Volume 2009.
39. Aflaki, S.; Hajikarimi, P.; Fini, E.H.; Zada, B. Comparing Effects of Biobinder with Other Asphalt Modifiers on Low-Temperature Characteristics of Asphalt. *J. Mater. Civ. Eng.* **2014**, *26*, 429–439. [[CrossRef](#)]
40. Sun, W.; Wang, H. Moisture effect on nanostructure and adhesion energy of asphalt on aggregate surface: A molecular dynamics study. *Appl. Surf. Sci.* **2020**, *510*, 145435. [[CrossRef](#)]
41. Liu, S.J.; Xu, T. Pyrolysis characteristics and kinetic analysis of magnesium hydroxide flame retardant asphalt. *Highway* **2021**, *66*, 341–347.
42. Liu, F.; Pan, B.; Li, Z.; Zhou, C.; Xu, S. Experimental Investigation on the Properties of Vulcanized Natural Rubber-Modified Asphalt Binder. *J. Transp. Eng. Part B Pavements* **2023**, *149*, 04023017. [[CrossRef](#)]

**Disclaimer/Publisher's Note:** The statements, opinions and data contained in all publications are solely those of the individual author(s) and contributor(s) and not of MDPI and/or the editor(s). MDPI and/or the editor(s) disclaim responsibility for any injury to people or property resulting from any ideas, methods, instructions or products referred to in the content.